IEEE Photonics Journal
An IEEE Photonics Society Publication

Open Access

Impact of the Order of Cavity Elements in All-Normal Dispersion Ring Fiber Lasers

Volume 7, Number 2, April 2015

O. V. Shtyrina
I. A. Yarutkina
A. Skidin
M. P. Fedoruk
S. K. Turitsyn, Senior Member, IEEE

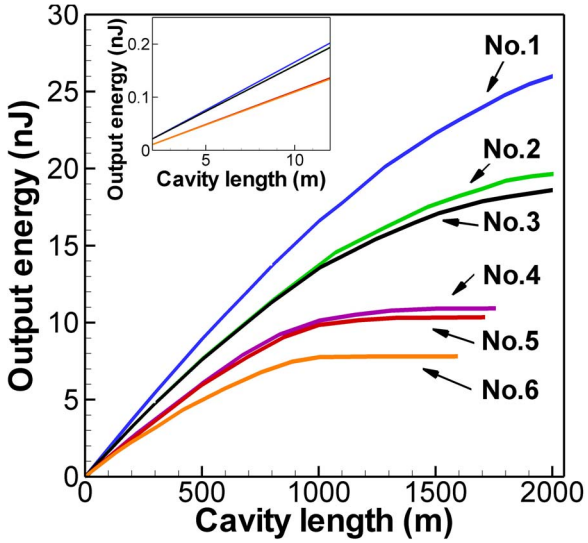

DOI: 10.1109/JPHOT.2015.2413591
1943-0655 © 2015 IEEE

IEEE photonics SOCIETY

IEEE

Impact of the Order of Cavity Elements in All-Normal Dispersion Ring Fiber Lasers

O. V. Shtyrina,[1,2] I. A. Yarutkina,[1,2] A. Skidin,[1,2] M. P. Fedoruk,[1,2] and S. K. Turitsyn,[1,3] *Senior Member, IEEE*

[1]Novosibirsk State University, 630090 Novosibirsk, Russia
[2]Institute of Computational Technologies, 630090 Novosibirsk, Russia
[3]Aston Institute of Photonic Technologies, Aston University, B4 7ET Birmingham, U.K.

DOI: 10.1109/JPHOT.2015.2413591

Manuscript received February 10, 2015; revised March 10, 2015; accepted March 13, 2015. Date of publication March 16, 2015; date of current version April 1, 2015. This work was supported by the Russian Science Foundation under Grant 14-21-00110. The work of S. K. Turitsyn was supported in part by the Ministry of Education and Science of the Russian Federation under Grant 14.B25.31.0003 and in part by the ERC project ULTRALASER. Corresponding author: I. A. Yarutkina (e-mail: i.yarutkina@gmail.com).

Abstract: Nonlinearity plays a critical role in the intra-cavity dynamics of high-pulse energy fiber lasers. Management of the intra-cavity nonlinear dynamics is the key to increase the output pulse energy in such laser systems. Here, we examine the impact of the order of the intra-cavity elements on the energy of generated pulses in the all-normal dispersion mode-locked ring fiber laser cavity. In mathematical terms, the nonlinear light dynamics in resonator makes operators corresponding to the action of laser elements (active and passive fiber, out-coupler, saturable absorber) non-commuting and the order of their appearance in a cavity important. For the simple design of all-normal dispersion ring fiber laser with varying cavity length, we found the order of the cavity elements, leading to maximum output pulse energy.

Index Terms: Ring lasers, fiber lasers.

1. Introduction

The classical theory of mode-locked lasers based on the distributed models such as Haus-Ginzburg-Landau equation assumes small fractional variations of pulse characteristics during the propagation through the cavity elements and, effectively, additive summation of changes over one transit of the resonator (see, e.g., [1]–[4] and references therein). However, in many modern high power or high intensity ultra-short pulse lasers generated field parameters, such as e.g., phase and bandwidth, are changed substantially during one round trip in the resonator, therefore, different theoretical treatment is required. The adequate theoretical approach in this case is the Poincare mapping over one round trip applied to transit intra-cavity dynamics [5]–[9]. The overall change of the field properties over the round trip $\widehat{T}_{RT}$ is a result of consecutive transformations at each element: $\widehat{T}_{RT} = \widehat{T_1}\ \widehat{T_2}\ \widehat{T_3}\ \widehat{T_4}\ldots$. Here $\widehat{T_k}$ denotes a complex transfer function (acting of the light envelope field) of various in-cavity elements, such as passive and active fiber, out-coupler, saturable absorber, optical filter, and so on. The overall resonator transfer operator $\widehat{T}_{RT}$ governs the radiation $A(t)$ transformation after one round trip evolution:

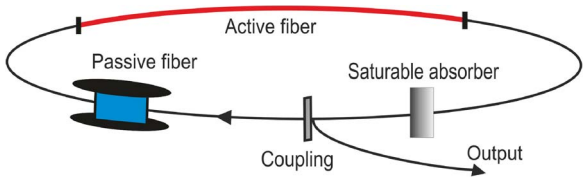

Fig. 1. Schematics of the ring laser cavity.

$A_{n+1} = \widehat{T}_{RT} A_n$. In the simplest case, an asymptotic (steady-state) shape of a generated pulse corresponds to a stable point of the Poincare mapping: $A_{n+1} = \widehat{T}_{RT} A_n = \exp(i\Lambda) A_n$.

One of the practically important challenges related to mode-locked lasers is generation of high pulse energy in the oscillator. This can be achieved by different means (see, e.g., references [4], [10]–[22] and literature and discussions therein). In particular, increase of the fiber laser cavity length to kilometer scale was actively studied in recent years as a method to generate high energy pulses [12]–[14], [16]–[19]. In general, the output pulse energy in mode-locked lasers depends on many variables that include the characteristics of intra-cavity devices, such as active/passive fibers, the saturable absorber, the output coupler etc. Also for system with strong nonlinear intra-cavity dynamics, pulse energy depends on the arrangement of these elements in the resonator. In this paper, we quantify the impact of the order of the resonator elements on generated pulse energy, considering, as a particular, albeit important example, all-normal dispersion ring cavity fiber laser.

2. Theoretical Analysis of Configurations of All-Normal Fiber Lasers

Let us consider the typical laser scheme depicted in Fig. 1. It is composed of the saturable absorber, passive and active fiber and the output coupler. To study impact of the order of cavity elements on generated pulse energy we, first, will examine different variants in which we change only the order of components while keeping all other parameters and characteristics the same. We compare pulse energy at the output of the system, right after out-coupler. Without loss of generality, we consider here the saturable absorber (SA) described by the standard simplified expression for the SA losses [9]

$$q(t) = \frac{q_0}{1 + P(t)/P_{\text{sat}}} \tag{1}$$

where t is the local time retarded by the corresponding number of the round trip delay time with respect to the real time, $q(t)$ is the SA saturating loss, q_0 is related to the modulation depth, P_{sat} is the SA saturation power, and $P(t)$ is the pulse power at the SA input. The energy losses in the saturable absorber are found using the standard formula [9]: $l_{\text{SA}} = -10\log_{10} \int (1 - q(t)) P(t) dt / \int P(t) dt$. Here, l_{SA} is expressed in dB. Obviously, $0 < l_{\text{SA}} < -10\log_{10}(1 - q_0)$. The energy loss at the saturable absorber l_{SA} is a functional of the power at the input of SA. This power, in turn, depends on the order the preceding elements.

Besides the configuration shown in Fig. 1, there are five more possible schemes of ring fiber lasers with the same cavity components. Let us introduce the following notations for the key system parameters: the passive fiber length L_P; the passive fiber losses α_P (expressed in dB/km); the saturable absorber losses (dependent on SA input power) l_{SA}; the output coupler (OC) parameter $R = E_{\text{OC}}/E_{\text{in\_OC}}$, where E_{OC} is the energy that remains in the laser cavity after the output coupler (output energy is $E_{\text{out}} = (1 - R) E_{\text{in\_OC}}$); and $E_{\text{in\_OC}}$ is the energy before the coupler.

We will denote each cavity configuration as a sequence of the components as they are arranged in the cavity. The following notation is used: AF and PF stand for the active and passive fibers, respectively; SA denotes the saturable absorber; and OC stands for the output coupler. For example, in the configuration AF-PF-SA-OC, the active fiber is followed by a

TABLE 1

List of configurations given in descending order of the output energy

	Configuration	Output energy, E_{out}
1	PF-AF-SA-OC	$E_{\text{AF}} \exp\left(-l_{\text{SA}}[P_{\text{out\_AF}}] \cdot 0.1 \ln 10\right) \cdot (1-R)$
2	AF-SA-PF-OC	$E_{\text{AF}} \exp\left[(-l_{\text{SA}}[P_{\text{out\_AF}}] - \alpha_P L_P) \cdot 0.1 \ln 10\right] \cdot (1-R)$
3	AF-PF-SA-OC	$E_{\text{AF}} \exp\left[(-l_{\text{SA}}[P_{\text{out\_AF}} \exp(-\alpha_P L_P)] - \alpha_P L_P) \cdot 0.1 \ln 10\right] \cdot (1-R)$
4	SA-PF-AF-OC	$E_{\text{AF}} \cdot (1-R)$
5	PF-SA-AF-OC	$E_{\text{AF}} \cdot (1-R)$
6	SA-AF-PF-OC	$E_{\text{AF}} \cdot \exp\left[-\alpha_P L_P \cdot 0.1 \ln 10\right] \cdot (1-R)$

passive fiber, and it, in turn, is followed by a saturable absorber, etc. For the sake of clarity, each representation of the cavity configuration is terminated by the coupler, where we take the output pulse energy for comparison of different schemes.

Let us first compare different configurations qualitatively and then verify the conclusions through direct numerical modeling. The qualitative consideration is based on the assumption that pulse energy after active fiber should be about the same in all configurations. This is, evidently, not true in all lasers, but as we demonstrate below, this assumption is supported by comparison with direct numerical modeling. In a particular case when the passive fiber is absent, we have just two possible configurations: AF-SA-OC and SA-AF-OC. The SA losses are minimal when the SA input power is at maximum (1). This means that it would be beneficial to place the saturable absorber right after the active fiber. Consequently, one can expect that the configuration AF-SA-OC (type 1) would generate the higher output energy than the configuration SA-AF-OC (type 2). It should be noted that the order of SA and OC in the cavity is important when the losses at the output coupler are large. In this case, the SA losses grow because of the saturation.

We would expect that the same arguments can be applied when the passive fiber is included and the order of the cavity devices leading to higher pulse energy is the one with the active fiber followed by a saturable absorber. Two configurations satisfy this condition: PF-AF-SA-OC and AF-SA-PF-OC. For the configuration PF-AF-SA-OC (1) $E_{\text{out}} = E_{\text{AF}}\exp[-l_{\text{SA}} \cdot 0.1\ln 10] \cdot (1-R)$, while for the configuration AF-SA-PF-OC (2) $E_{\text{out}} = E_{\text{AF}}\exp[(-l_{\text{SA}} - \alpha_P L_P) \cdot 0.1\ln 10] \cdot (1-R)$. Assuming that E_{AF} is close in value [15] for the both considered schemes, we can conclude that configuration (1) should have the higher output pulse energy compared to (2), because of higher input power at SA element. We would like to stress again, that this is just a qualitative consideration based on the quite restrictive assumption, that yet has to be confirmed by direct numerical modeling.

The configuration AF-PF-SA-OC (3) should lead to the lower energy than (2), because SA losses l_{SA} for (3) are larger than for (2). The configurations PF-SA-AF-OC, SA-AF-PF-OC, SA-PF-AF-OC can be ordered (in terms of expected output pulse energy) in a similar way. The expressions for the output pulse energy for each configuration are listed in Table 1. The columns in Table 1 represent, from left to right, the configuration number, the scheme description and the expression for the corresponding output energy. Note that l_{SA} is a functional of the SA input power. The configurations in Table 1 are given in a descending order of the output pulse energy values.

In case of a long cavity (i.e. when the passive fiber length increases) the distinction between each of six configuration may be substantial. On the contrary, for short cavities the following relations hold:

$$E_{\text{out}}^{(1)} \approx E_{\text{out}}^{(2)} \approx E_{\text{out}}^{(3)} > E_{\text{out}}^{(4)} \approx E_{\text{out}}^{(5)} \approx E_{\text{out}}^{(6)}.$$

3. Results of Numerical Simulation

Below we verify our qualitative analysis by the direct numerical modeling of the configurations listed in Table 1. The mathematical modeling was based on the standard scalar nonlinear Schrödinger equation solved using split-step Fourier method and modified for the active fiber by

TABLE 2

Fiber laser parameters

Element	Parameter	Value
Active Er-doped fiber [8]	Length L_A	2 m
	2nd order dispersion β_2	76.9 fs^2/mm
	3d order dispersion β_3	168 fs^3/mm
	Nonlinear parameter γ	9.32 1/W/km
	Gain bandwidth Λ_g	50 nm
	Saturation power P_{satG}	20 mW
	Small signal gain g_A	Variable
Passive fiber OFS-980 [8]	Length L_P	Variable
	2nd order dispersion β_2	4.5 fs^2/mm
	3d order dispersion β_3	109 fs^3/mm
	Nonlinear parameter γ	2.1 1/W/km
Saturable absorber [9]	Modulation depth q_0	10%
	Saturation power P_{sat}	3.69 W
System	Fiber losses α_A, α_P	0.2 dB/km
	Output losses $1 - R$	About 90%

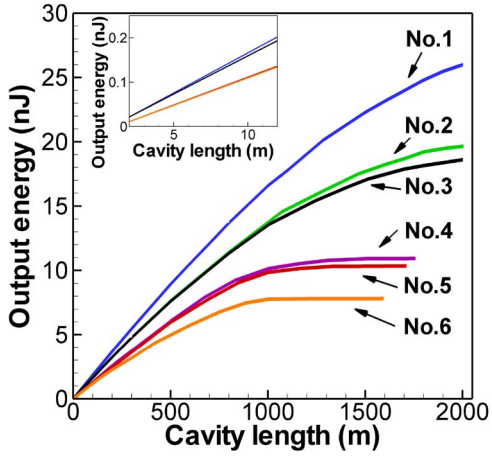

Fig. 2. Output energy dependence on the cavity length for different laser configurations.

the gain term [9], [20], [23]. In this model, we did not take into account the effect of nonlinear evolution of polarization; however, it is known [9], [10] that the scalar model with properly adjusted effective saturable absorber (e.g., due to the nonlinear evolution of polarization) describes well properties of broad classes of lasers. We use the white Gaussian noise as an initial distribution. The details of modeling were described in [23]. The fiber laser parameters are presented in Table 2.

The length of the laser cavity was varied in modeling from 2 meters (no passive fiber) to several kilometers. Fig. 2 depicts the output pulse energy dependence on the cavity length for the constant small signal gain $g_A L_A = 10.8$ dB. We observe that the variation of the laser configuration from 6 to 1 increases the pulse energy from 0.11 nJ to 0.15 nJ in the case of the cavity length of 2 m, and from 7.7 nJ to 26.3 nJ for the cavity length of 2002 m. The observed energy saturation with increase of the cavity length for cases 4, 5, and 6 is due to increase of the overall saturable absorber losses. The observed order of the output energy values for different schemes agrees well with the qualitative analysis given above for each configuration listed in Table 1. As one can see from Fig. 2, the efficiency of the optimal configuration improves with the increase of the total cavity length. Note that our results are in line with the approaches to the optimization of different laser configuration used in practice (see, for example, [24] where similar design rules are applied to the laser cavity comprising negative and positive dispersion fiber spans and bulk polarization control elements).

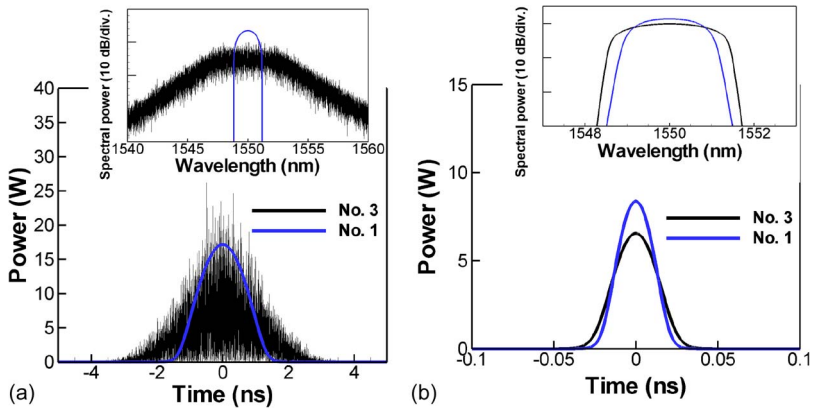

Fig. 3. Stable pulses generated in the cavities including (a) 2000 m and (b) 10 m of the passive fiber. The blue curve corresponds to configuration 1, and the black curve corresponds to configuration 3. Corresponding insets show the generated pulse spectra.

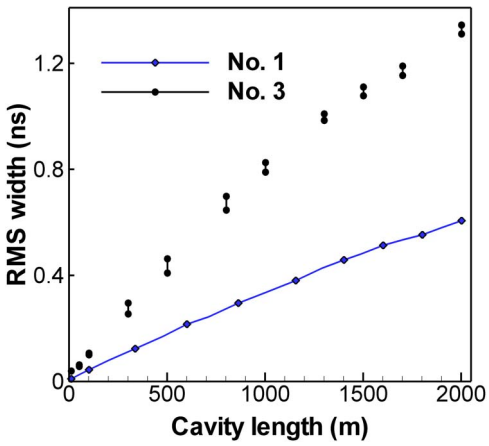

Fig. 4. Dependence of RMS pulse width on the cavity length (up to 50 m) for configurations 1 (blue curve) and 3 (black curve).

We would like to point out that the advantage of one scheme over the other is not only in terms of the output pulse energy. Fig. 3 shows the comparison of pulse shapes for configuration 1 from Table 1 and configuration 3 studied thoroughly in [23]. The generated pulse shapes for stable regimes are shown for the cavities with 2000 m (a) and 10 m (b) length of passive fiber. The insets in Fig. 3 depict the corresponding pulse spectra.

The pulse generated in scheme 1 reaches a smooth shape approximately after 6000 round trips, while the pulse generated in cavity 3 has noisy oscillation components even after 120 000 round trips [23]. The change of the laser configuration not only allows an increase in the output pulse energy, but also may lead to better quality (more coherent) pulses. This analysis will be presented in more details elsewhere.

Fig. 4 depicts the root-mean square (RMS) pulse width dependence on the cavity length for configurations 1 (blue curve) and 3 (black curve). The black intervals show the variance of the results corresponding to different realizations of the initial noise distribution [23]. Figs. 3 and 4 demonstrate that configuration 1 allows one to generate shorter pulses with the higher pulse energy.

Before this point we considered the same small signal gain in the cavity. Now we relax this condition and study the generation of stable single pulses without assumption of the same total small signal gain. This means that pulse energy is limited only by the nonlinear effects and the

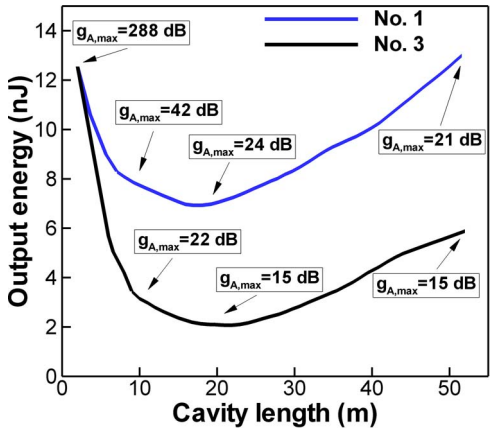

Fig. 5. Dependence of the output energy on the cavity length for configurations 1 (blue curve) and 3 (black curve) for the maximum small signal gain that allows one to achieve the stable single-pulse regime.

requirement of the stable single pulse generation in each configuration. In this case, we consider a single pulse generation regime to be "stabilized" when the relative variation of emerging pulse energy does not exceed 10^{-3} from one round trip to another, similar to [23].

Fig. 5 shows the dependence of the output pulse energy on the cavity length (now for the length is limited by 50 m, that is why the absolute output energies are smaller compared to Fig. 2) for configurations 1 and 3 with varying small signal gain that is limited by the requirement of the stable single-pulse generation. It can be seen that configuration 1 gives the higher output pulse energy for any considered cavity length. The numerically computed curves shown in Fig. 5 are in agreement with the theoretical expression derived in [15] with the value of small signal gain corresponding to the end of stable generation. We observe the improved steady-state generation range for scheme 1, which can be explained by the more efficient mode-locking for this optimal configuration. The numerical modeling results presented in Figs. 2 and 5 (for relatively short fiber length, up to 50 m) confirm our theoretical predictions. The efficiency of the optimal configuration is increasing even further with the increase of the total cavity length.

4. Conclusions

In this study, we have presented the theoretical analysis of optimal order of elements in the cavity of all-normal dispersion mode-locked fiber lasers. Given the results obtained above it can be concluded that to maximize the output energy for a system that contains a device that has larger losses for the smaller input power (e.g., saturable absorber), this device should be placed immediately after the gain medium and should be followed by the output coupler. Our results generalize previous research on optimal position of an optical filter in a cavity of all-normal dispersion fiber laser [25].

The advantage of the optimal order of elements in a cavity becomes significant for fiber lasers with ultra-long resonators. For the simple design of all-normal dispersion ring fiber laser with varying cavity length we found the order of the cavity elements leading to maximum output pulse energy. It has been shown that to achieve the maximum output energy it is necessary to place the saturable absorber after the gain medium and, in turn, place the output coupler after the saturable absorber. The optimization of laser performance through right ordering of the cavity elements is applied to almost all laser systems where nonlinear intra-cavity light dynamics makes action of elements non-commuting. Of course, the presented theoretical analysis should be considered only as a first step in more accurate numerical and experimental optimization studies, due to complex nonlinear intra-cavity dynamics characteristic for high-energy pulse laser systems. Our approach can be generalized to dispersion-managed and more complex laser systems.

References

[1] H. A. Haus, "Theory of mode locking with a slow saturable absorber," *IEEE J. Quantum Electron.*, vol. QE-11, no. 9, pp. 736–746, Sep. 1975.

[2] H. A. Haus, "Mode-locking of lasers," *IEEE J. Sel. Topics Quantum Electron.*, vol. 6, no. 6, pp. 1173–1185, Nov./Dec. 2000.

[3] O. E. Martinez, R. L. Fork, and J. P. Gordon, "Theory of passively mode-locked lasers for the case of a nonlinear complex-propagation coefficient," *J. Opt. Soc. Amer. B*, vol. 2, no. 5, pp. 753–760, May 1985.

[4] P. Grelu and N. Akhmediev, "Dissipative solitons for mode-locked lasers," *Nature Photon.*, vol. 6, no. 2, pp. 84–92, Jan. 2012.

[5] T. Brabec, C. Spielmann, and F. Krausz, "Mode locking in solitary lasers," *Opt. Lett.*, vol. 16, no. 24, pp. 1961–1963, Dec. 1991.

[6] B. G. Bale, J. N. Kutz, A. Chong, W. H. Renninger, and F. W. Wise, "Spectral filtering for mode locking in the normal dispersive regime," *Opt. Lett.*, vol. 33, no. 9, pp. 941–943, May 2008.

[7] B. G. Bale, S. Boscolo, J. N. Kutz, and S. K. Turitsyn, "Intracavity dynamics in high-power mode-locked fiber lasers," *Phys. Rev. A*, A 81, Mar. 2010, Art. ID. 033828.

[8] B. Oktem, C. Ülgüdür, and F. Ömer Ilday, "Soliton-similariton fibre laser," *Nature Photon.*, vol. 4, pp. 307–311, Mar. 2010.

[9] B. G. Bale, O. G. Okhotnikov, and S. K. Turitsyn, "Modeling and technologies of ultrafast fiber lasers," in *Fiber Lasers*, O. G. Okhotnikov, Ed. Weinheim, Germany: Wiley-VCH Verlag GmbH Co., 2012.

[10] F. W. Wise, A. Chong, and W. H. Renninger, "High-energy femtosecond fiber lasers based on pulse propagation at normal dispersion," *Laser Photon. Rev.*, vol. 2, no. 1/2, pp. 58–73, Apr. 2008.

[11] V. L. Kalashnikov and A. Apolonski, "Chirped-pulse oscillators: A unified standpoint," *Phys. Rev. A*, vol. A-79, Apr. 2009, Art. ID. 043829.

[12] S. Kobtsev, S. Kukarin, and Y. Fedotov, "Ultra-low repetition rate mode-locked fiber laser with high-energy pulses," *Opt. Exp.*, vol. 16, no. 26, pp. 21 936–21 941, Dec. 2008.

[13] E. J. R. Kelleher *et al.*, "Generation and direct measurement of giant chirp in a passively mode-locked laser," *Opt. Lett.*, vol. 34, no. 22, pp. 3526–3528, Nov. 2009.

[14] B. N. Nyushkov *et al.*, "Generation of 1.7-μJ pulses at 1.55 μm by a self-modelocked all-fiber laser with a kilometers-long linear-ring cavity," *Laser Phys. Lett.*, vol. 7, no. 9, pp. 661–665, 2010.

[15] S. K. Turitsyn, "Theory of energy evolution in laser resonators with saturated gain and non-saturated loss," *Opt. Exp.*, vol. 17, no. 14, pp. 11898–11904, Jul. 2009.

[16] V. I. Denisov, B. N. Nyushkov, and V. S. Pivtsov, "Self-mode-locked all-fibre erbium laser with a low repetition rate and high pulse energy," *Quantum Electron.*, vol. 40, no. 1, pp. 25–27, 2010.

[17] N. Li *et al.*, "Cavity-length optimization for high energy pulse generation in a long cavity passively mode-locked all-fiber ring laser," *Appl. Opt.*, vol. 51, no. 17, pp. 3726–3730, Jun. 2012.

[18] A. Boucon *et al.*, "Noise-like pulses generated at high harmonics in a partially-mode-locked km-long Raman fiber laser," *Appl. Phy. B*, vol. 106, no. 2, pp. 283–287, Feb. 2012.

[19] Z. Q. Luo *et al.*, "Raman fiber laser harmonically mode-locked by exploiting the intermodal beating of CW multimode pump source," *Opt. Exp.*, vol. 20, no. 18, pp. 19 905–19 911, Aug. 2012.

[20] T. Schreiber, B. Ortaç, J. Limpert, and A. Tünnermann, "On the study of pulse evolution in ultra-short pulse mode-locked fiber lasers by numerical simulations," *Opt. Exp.*, vol. 15, no. 13, pp. 8252–8262, Jun. 2007.

[21] X. H. Li *et al.*, "Long cavity passively mode-locked fiber ring laser with high-energy rectangular-shape pulses in anomalous dispersion regime," *Opt. Lett.*, vol. 35, no. 19, pp. 3249–3251, Oct. 2010.

[22] X. H. Li *et al.*, "Wavelength switchable and tunable all-normal-dispersion Yb-doped mode-locked fiber laser based on single-wall carbon nanotubes wall paper," *IEEE Photon. J.*, vol. 4, no. 1, no. 4, pp. 234–241, Feb. 2012.

[23] I. A. Yarutkina, O. V. Shtyrina, M. P. Fedoruk, and S. K. Turitsyn, "Numerical modeling of fiber lasers with long and ultra-long ring cavity," *Opt. Exp.*, vol. 21, no. 10, pp. 12 942–12 950, May 2013.

[24] K. Tamura, C. R. Doerr, L. E. Nelson, H. A. Haus, and E. P. Ippen, "Technique for obtaining high-energy ultrashort pulses from an additive-pulse mode-locked erbium-doped fiber ring laser," *Opt. Lett.*, vol. 19, pp. 46–48, Jan. 1994.

[25] C. M. Ouyang *et al.*, "Position effect of spectral filter on properties of highly chirped pulses in an all-normal-dispersion fiber laser," *IEEE J. Quantum Electron.*, vol. 45, no. 10, pp. 1284–1288, Oct. 2009.